

Population Genomic Structure and Recent Evolution of *Plasmodium knowlesi*, Peninsular Malaysia

Suzanne E. Hocking, Paul C.S. Divis, Khamisah A. Kadir, Balbir Singh, David J. Conway

Most malaria in Malaysia is caused by *Plasmodium knowlesi* parasites through zoonotic infection from macaque reservoir hosts. We obtained genome sequences from 28 clinical infections in Peninsular Malaysia to clarify the emerging parasite population structure and test for evidence of recent adaptation. The parasites all belonged to a major genetic population of *P. knowlesi* (cluster 3) with high genomewide divergence from populations occurring in Borneo (clusters 1 and 2). We also observed unexpected local genetic subdivision; most parasites belonged to 2 subpopulations sharing a high level of diversity except at particular genomic regions, the largest being a region of chromosome 12, which showed evidence of recent directional selection. Surprisingly, we observed a third subpopulation comprising *P. knowlesi* infections that were almost identical to each other throughout much of the genome, indicating separately maintained transmission and recent genetic isolation. Each subpopulation could evolve and present a broader health challenge in Asia.

All endemic human malaria parasite species originated as zoonotic crossover infections from nonhuman primates (1–3) and now cause approximately half a million human deaths annually (4). Until recently, zoonotic malaria was considered to be very rare, but original findings in Malaysia (5,6) and subsequent surveys elsewhere have revealed that many human malaria cases in Southeast Asia are caused by the macaque parasite *Plasmodium knowlesi* (7). This parasite species now causes almost all malaria in Malaysia (4) and is responsible for clinical cases throughout Southeast Asia, where the distributions of macaque reservoir hosts and mosquito vectors overlap with human populations (8). As several

countries in Southeast Asia are working toward eliminating malaria, *P. knowlesi* represents a special public health challenge. Because of the presence of wild reservoir hosts, elimination of *P. knowlesi* is unlikely, and the problem will deepen if the parasite adapts or environments change to enable more effective transmission between humans (9). Of particular concern, numbers of cases each year are continuing to increase (4), and intensive surveillance in particular areas indicates this increase is not attributable to ascertainment bias (10).

Population genetic studies are essential to determining whether recent parasite adaptation has occurred, which might reflect ongoing evolution that is likely to affect the epidemiology. The *P. knowlesi* parasite has a ≈ 25 megabase genome of 14 chromosomes (11,12), haploid in blood stage infections and recombining in a brief diploid stage after male and female parasites mate in the mosquito vector, so informative studies require analysis of loci throughout the genome. Understanding of *P. knowlesi* population genetics has been gained by microsatellite genotyping (13,14) and whole-genome sequencing (15,16). In Malaysian Borneo, *P. knowlesi* consists of 2 genetically divergent populations (termed clusters 1 and 2) associated with different reservoir hosts: cluster 1 with long-tailed macaques (*Macaca fascicularis*) and cluster 2 with pig-tailed macaques (*M. nemestrina*) (14). In Peninsular Malaysia, on the mainland of Asia, a different genetic subpopulation of *P. knowlesi* exists. This subpopulation was initially indicated by comparing genome sequences of a few old laboratory isolates from Peninsular Malaysia with genome sequences of recent clinical samples from Borneo (15), and by comparing sequences of 2 genes in clinical samples from both areas (17). Subsequent multi-locus microsatellite analysis of recent clinical cases of *P. knowlesi* infection from Peninsular Malaysia has confirmed that all cases are attributable to the cluster 3 type (13).

Author affiliations: London School of Hygiene and Tropical Medicine Department of Infection Biology, London, UK (S.E. Hocking, D.J. Conway); Universiti Sarawak Malaysia Malaria Research Centre, Kota Samarahan, Malaysia (P.C.S. Divis, K.A. Kadir, B. Singh, D.J. Conway)

DOI: <https://doi.org/10.3201/eid2608.190864>

Experimental studies have been conducted on only a few strains of *P. knowlesi*, isolated many years ago and maintained in laboratory monkeys (18). Genome sequencing has revealed these strains to be of the cluster 3 type (13,15), and one of them has been adapted to in vitro culture in human erythrocytes, using 2 independent approaches involving culture with mixtures of macaque and human erythrocytes before growth in human erythrocytes alone (19,20). The short-term adaptability of this single strain is further illustrated by selection for culture in long-tailed macaque erythrocytes, which was associated with the loss of a specific ligand gene needed for invading human erythrocytes (21). These examples from laboratory observations strongly suggest that highly diverse natural parasite populations are likely to adapt to changing conditions.

All of the separately occurring *P. knowlesi* populations might evolve and emerge to present an even more serious public health challenge than already realized. To determine the population genetic substructure within *P. knowlesi* locally, we analyzed recent clinical samples from patients with *P. knowlesi* infection in Peninsular Malaysia by using whole-genome sequencing.

Materials and Methods

We collected heparinized venous blood samples of up to 10 mL from 56 patients with *P. knowlesi* malaria at 5 hospitals in Peninsular Malaysia during February 2016–January 2018 (Figure 1; Appendix 1 Table, <https://wwwnc.cdc.gov/EID/article/26/8/19-0864-App1.pdf>), after obtaining written informed consent from each patient. The study was approved by the Medical Research and Ethics Committee of the Malaysia Ministry of Health and by the Ethics Committee of the London School of Hygiene and Tropical Medicine.

We depleted leukocytes by passing each blood sample through a CF11 cellulose column to increase the proportion of parasite compared with host DNA. We extracted genomic DNA by using QIAamp DNA Mini kits (QIAGEN, <https://www.qiagen.com>) and confirmed that all contained only *P. knowlesi* by using nested PCR assays, testing for all locally known malaria parasite species (22). We lyophilized genomic DNA before transport to the United Kingdom, then dissolved the DNA in 30 μ L of nuclease-free water and quantified it on a spectrophotometer by using the Quant-iT PicoGreen dsDNA Assay Kit (Thermo Fisher Scientific, <https://www.thermofisher.com>). We processed samples containing ≥ 300 ng of DNA for sequencing. We performed

paired-end short-read genome sequencing by using Illumina MiSeq version 3 kits on the MiSeq platform (Illumina, <https://www.illumina.com>) with a read length of 300 bp, and aligned reads to the *P. knowlesi* PKNH 2.0 reference genome sequence (Appendix 1). After assembly and quality filtering, data from 28 clinical case samples were available for downstream analysis, representing samples from 5 hospitals in Peninsular Malaysia (Figure 1). For comparison with samples from elsewhere, we retrieved Illumina short reads from previous studies (15,16,23) and assembled them by using the identical pipeline as we had for the newly sequenced samples.

We masked from analysis parts of the genome to which short reads are difficult to uniquely map, including the subtelomeres and the multicopy *kir* and *SICAvar* gene families (Appendix 1). We called single-nucleotide polymorphisms (SNPs) by using



Figure 1. Locations of hospitals in peninsular Malaysia from which clinical *Plasmodium knowlesi* infections were sampled and sequenced in the states of Perak (Taiping and Sungai Siput), Kelantan (Gua Musang), and Pahang (Kuala Lipis and Temerloh). Of 56 infection samples processed through leukocyte depletion and subsequent DNA extraction, 32 had sufficient quantity and purity of *P. knowlesi* DNA for Illumina sequencing (<https://www.illumina.com>), of which 28 yielded high coverage genomewide sequence for population genomic analysis (sample and sequencing details listed in Appendix 1 Table, <https://wwwnc.cdc.gov/EID/article/26/8/19-0864-App1.pdf>).

a full repertoire of *P. knowlesi* genome sequences, including the 28 new sequenced infection samples from Peninsular Malaysia with high read coverage obtained in this study, as well as 74 previous samples from Malaysian Borneo (40 from cluster 1 and 34 from cluster 2) and 5 laboratory isolates (107 in total) (15,16,23). The procedures and parameters we used are comparable to those used for other original studies of *P. knowlesi* conducted previously (15,16) and to those used in population studies on endemic human malaria parasites, such as *P. falciparum*, that have much less diversity than *P. knowlesi* (15,24).

We used the packages adegenet (<https://github.com/thibautjombart/adegenet/wiki>) (25) and pegas (<https://cran.r-project.org/web/packages/pegas/index.html>) (26) in the R statistical framework to conduct principal component analysis and generate neighbor-joining trees by using an SNP-based pairwise genetic distance matrix. For population structure analysis, we used the package PopGenome (27) to calculate nucleotide diversity, within-population Tajima's D indices, and between-population fixation indices (F_{ST}). For sliding-window analysis genome-wide, we calculated nucleotide diversity in nonoverlapping 50-kb windows. To scan for genes that might be under balancing selection, we calculated Tajima's D on a gene-by-gene basis and excluded genes with <3 SNPs from analysis. We calculated F_{ST} values between each of the major parasite clusters for all individual SNPs across the genome with a minor allele frequency of $\geq 10\%$, and we calculated mean values in all nonoverlapping sliding windows of 500 consecutive SNPs across the genome.

We performed a scan for loci under recent positive selection by identifying SNPs with an allele associated with extended haplotype homozygosity, using the R package rehh (28) and applying the default setting assumption that common alleles are more likely to be ancestral. We calculated the standardized integrated haplotype score ($|iHS|$) for biallelic SNPs with no missing calls and with a minor allele frequency of $\geq 10\%$. We set SNPs with $|iHS|$ values in the top 0.01% as core SNPs, around which we identified putative windows of selection by using the extended haplotype homozygosity (EHH) score, plotted until the EHH signal declined to < 0.05 on each side. We merged overlapping windows of EHH containing some of the same SNPs to produce a contiguous overall putative selection window for that region, and we considered any gaps of > 20 kb between SNPs with elevated $|iHS|$ values to break a putative window of selection.

Results

Genomic Diversity of Different *P. knowlesi* Subpopulations

We successfully obtained paired-end short read Illumina genome sequences with high-read depth mapping to the *P. knowlesi* reference sequence from 28 *P. knowlesi* clinical case samples (Appendix 1) gathered from hospitals at 5 locations in Peninsular Malaysia (Figure 1). Analysis of these new infection samples together with previous sequences from infections in Malaysian Borneo enabled 994,761 SNPs to be initially called, of which 40,934 SNPs were removed because they were in genomic regions with generally unreliable short-read mapping (*kir* and *SICAvar* genes and subtelomeres), resulting in a total of 953,827 SNPs throughout the rest of the genome. After filtering out SNPs that had missing data in $> 10\%$ of individual infection samples, we included 474,109 high-quality SNPs in subsequent analysis (Appendix 2 Datasheet 1, <https://wwwnc.cdc.gov/EID/article/26/8/19-0864-App2.xlsx>).

We generated a neighbor-joining tree by using pairwise genetic distances among individual *P. knowlesi* infection samples, which considered most nucleotide calls for all SNPs within each infection sample (Figure 2, panel A). The tree showed that all of the 28 samples from Peninsular Malaysia belonged to a genetic population (cluster 3) divergent from those in Malaysian Borneo (clusters 1 and 2). These new clinical samples from Peninsular Malaysia clustered with the old laboratory isolates (mostly from Peninsular Malaysia) that were sequenced previously and had initially indicated the existence of a third major genetic population within this species (15). The overall genomewide nucleotide diversity (π) among the new cluster 3 samples was 4.13×10^{-3} (the allele frequency spectrum is shown in Appendix 1 Figure 1), broadly similar to that for cluster 1 and higher than for cluster 2 (Figure 2, panel B). Differences between clusters 1 and 2 have been examined in detail in original analysis of parasites from Malaysian Borneo (16), and higher population genomic diversity within *P. knowlesi* has been noted in comparison with endemic malaria parasite species *P. vivax* and *P. falciparum* (15).

Low Levels of Diversity within Individual Clinical Infections

Although all of the *P. knowlesi* clinical isolates were genotypically distinct from each other as indicated by considerable pairwise differences, most of them contained minimal within-infection sequence diversity, as indicated by the high values of the genomewide within-isolate fixation index F_{WS} (Figure 3). Of the 28

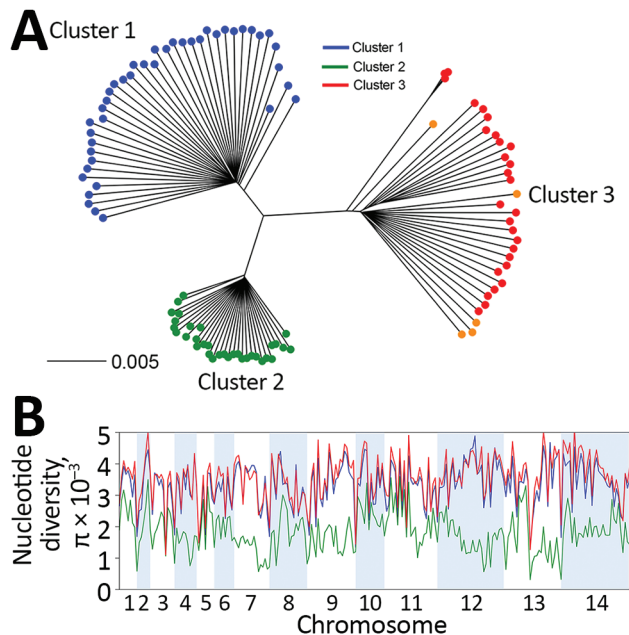


Figure 2. Genomewide analysis of diversity in *Plasmodium knowlesi* clinical samples from Peninsular Malaysia compared with samples from elsewhere. A) Neighbor-joining tree based on a pairwise genetic distance matrix between individual *P. knowlesi* infection samples for the 28 new clinical samples from Peninsular Malaysia (shown in red), 5 previously sequenced laboratory isolates (shown in orange), most of which were originally isolated from Peninsular Malaysia many years ago (15), and 74 samples from Malaysian Borneo that grouped into separate subpopulation clusters (cluster 1 shown in blue, cluster 2 in green) (15,16,23). All the clinical isolate samples from Peninsular Malaysia grouped into cluster 3 together with the laboratory isolates. The distance matrix is based on the proportion of all single-nucleotide polymorphisms (SNPs) showing differences between each infection sample (scale bar shows branch length for 0.5% of SNPs differing); most reads within each infection sample determine the allele scored for each SNP. B) Genomewide scan of nucleotide diversity (π) for *P. knowlesi* among the clinical isolates in Peninsular Malaysia (cluster 3, shown in red), compared with diversity observed in the subpopulations in Malaysian Borneo (clusters 1 and 2). The sliding window plot shows values of nucleotide diversity for nonoverlapping windows of 50 kb in each of the 14 chromosomes.

cluster 3 clinical isolates from Peninsular Malaysia in our study, only 4 were clearly mixed (with F_{ws} values <0.95). This low proportion of mixed genotype infections was similar to that observed for the different *P. knowlesi* subpopulations (clusters 1 and 2) in Malaysian Borneo (Figure 3).

Population Genetic Substructure of *P. knowlesi* in Peninsular Malaysia

Analysis of SNP allele frequencies genomewide confirmed that the *P. knowlesi* cluster 3 population in Peninsular Malaysia is highly divergent from each of the separate clusters 1 and 2 in Malaysian Borneo

(Figure 4). Comparison of cluster 3 with cluster 1 reveals a genomewide mean F_{ST} values of 0.32 (with 3,713 SNPs being at complete fixation), whereas comparison of cluster 3 with cluster 2 reveals a genomewide mean F_{ST} value of 0.42, (with 6,738 SNPs being at complete fixation) (Figure 4; Appendix 1 Figure 2). We observed a high consistency across the genome in the level of divergence when comparing cluster 3 with cluster 1 (Figure 4, panel A), but more variation across the genome was apparent in the comparison between cluster 3 and cluster 2 (Figure 4, panel B). This finding is attributable to a previously described mosaic pattern of diversity across the genome of cluster 2 (16), which contributes to greater genomewide heterogeneity in divergence between clusters 1 and 2 in Malaysian Borneo (Figure 4, panel C) than between either of these and cluster 3 in Peninsular Malaysia.

The distance matrix-based neighbor-joining tree indicated internal branching of the *P. knowlesi* cluster 3 clinical samples from Peninsular Malaysia into 3 different subclusters (Figure 2, panel A). To examine this branching further, we focused the principal component analysis on the clinical samples from Peninsular Malaysia alone, which showed that they formed 3 groups (Figure 5, panel A). The smallest group contained 3 of the samples (GMK03, TPK03, and KLK12) separated from the rest along principal component 1 (which explained 10.5% of overall variation), whereas

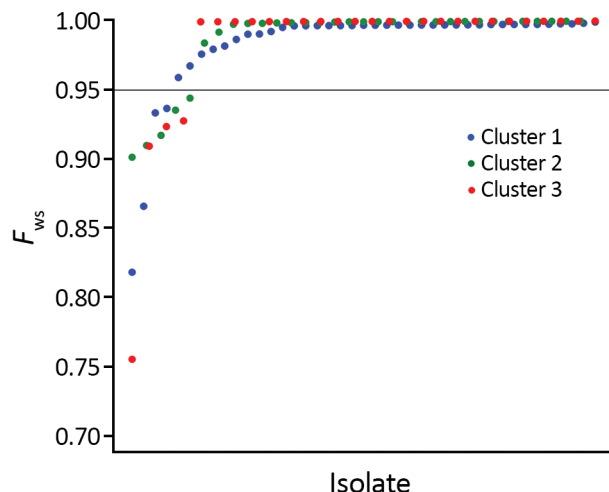
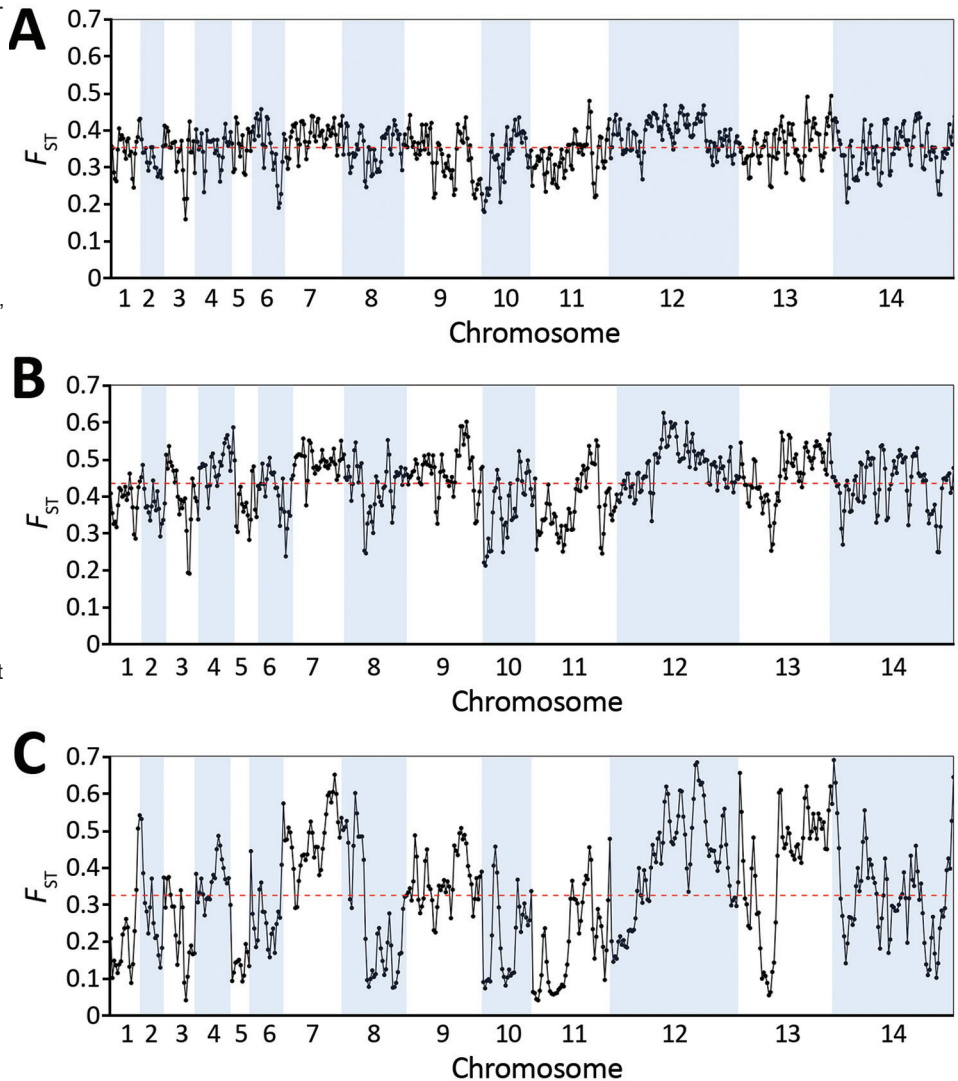


Figure 3. Low levels of diversity within individual *Plasmodium knowlesi* clinical infections from Malaysia as indicated by the high values of the genomewide within-isolate fixation index F_{ws} (potential range 0–1). A value of ≥ 0.95 is generally taken to indicate an infection dominated by a single genotype, whereas values <0.95 indicate infections that are clearly genotypically mixed. Each point shows the value for an individual infection sample; only 4 of the 28 cluster 3 clinical isolates from Peninsular Malaysia are clearly mixed (similar to the proportions observed in infections with the cluster 1 and 2 types in Malaysian Borneo).

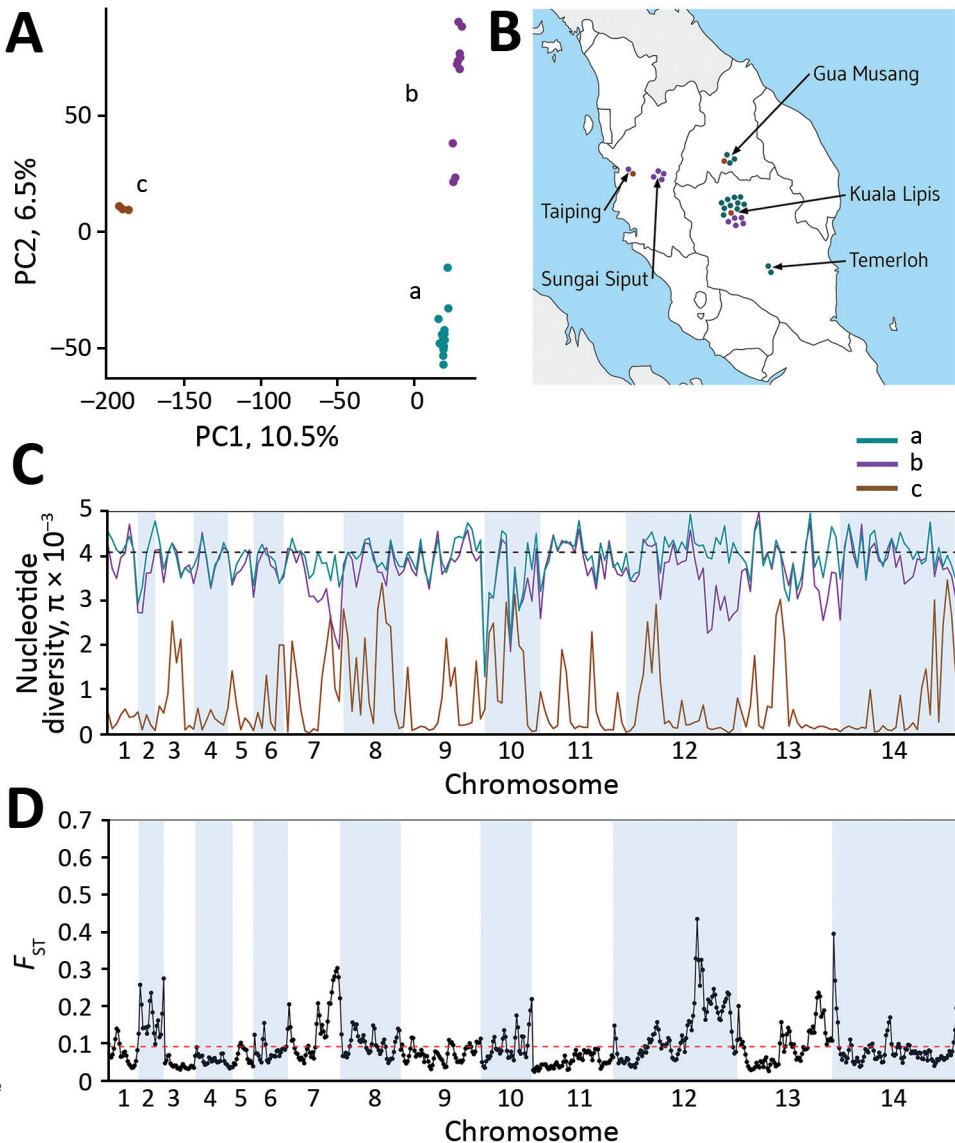
Figure 4. Genomewide between-population fixation index (F_{ST}) scan of divergence between *Plasmodium knowlesi* in Peninsular Malaysia sampled in this study (cluster 3) and the major subpopulations previously sampled in Malaysian Borneo (clusters 1 and 2). All single-nucleotide polymorphisms (SNPs) with overall allele frequencies $\geq 10\%$ were included, and the solid points show values for analysis windows containing 500 consecutive SNPs, centered by the midpoint of each sequential window and overlapping by 250 SNPs. The red dashed line on each plot shows the genomewide mean value for all analyzed SNPs across the genome. A) The level of divergence between cluster 3 in Peninsular Malaysia and cluster 1 in Malaysian Borneo does not differ greatly throughout the genome (mean F_{ST} value 0.32). B) Divergence between cluster 3 in Peninsular Malaysia and cluster 2 in Malaysian Borneo is slightly higher (mean F_{ST} value 0.42) and shows more heterogeneity between genomic regions because of mosaic structure of diversity in cluster 2 (as explained by panel C). C) Divergence between clusters 1 and 2 in Malaysian Borneo, showing marked heterogeneity across the genome that explains most of the moderate heterogeneity shown in panel B, attributable to a mosaic structure of diversity within cluster 2, as previously reported (16).



the 2 other groups were less tightly separated along principal component 2 (which explained 6.5% of overall variation) (Figure 5, panel A). These 3 groups existing within *P. knowlesi* cluster 3 in Peninsular Malaysia are considered as subpopulations, designated in this article as subclusters A (15 of the infections), B (10 infections), and C (3 infections), which are also apparent in neighbor-joining analysis of the cluster 3 samples alone (Appendix 1 Figure 3). These different parasite genetic subclusters are not separated geographically within Peninsular Malaysia, each being detected from multiple sites (Figure 5, panel B), and the hospital with the largest sample size (in Kuala Lipis) had infections of all 3 subclusters. Moreover, infections of the different subcluster types were not temporally aggregated (Appendix 1 Table).

The most divergent of these types (subcluster C) consisted of infections that were highly related to each other, virtually identical in many parts of the genome (Figure 5, panel C). This finding is remarkable because each of these cases were sampled from different states within Peninsular Malaysia (Figure 4, panel B). Although subclusters A and B had similar levels of nucleotide diversity to each other, sliding-window analysis indicated a few genomic regions in which subcluster B has lower diversity than subcluster A (e.g., in a region covering half of chromosome 12) (Figure 5, panel C). Genomewide scan of differentiation between subclusters A and B by sliding-window F_{ST} analysis showed peaks of high differentiation against a background of low differentiation in most of the genome (Figure 5, panel D). The regions that

Figure 5. *Plasmodium knowlesi* cluster 3 clinical isolates forming genomic subpopulations that co-occur locally, Peninsular Malaysia. A) Principal component analysis of the 28 cluster 3 *P. knowlesi* clinical isolates from Peninsular Malaysia, showing clustering into 3 groups: subclusters A (15 isolates), B (10 isolates), and C (3 isolates). The assignment of all samples to these 3 subclusters is completely consistent with their placement in the within-cluster 3 branching of the neighbor-joining tree based on the pairwise distance matrix (Figure 2, panel A). The first principal component accounts for 10.5% of overall variation and separated subcluster 3 from the others, whereas the second principal component accounts for 6.5% of overall variation and separated subclusters A and B. B) Each of the cluster 3 *P. knowlesi* subclusters was detected at multiple sites within peninsular Malaysia (points shown at each of the 5 sampling sites show individual infections with colors for the different subclusters as in panel A). The site with most samples had all 3 subclusters co-occurring locally. C) Genomewide scan of diversity shows that the subcluster C samples are virtually identical in large parts of the genome, whereas subclusters A and B are both highly diverse throughout the genome, with only a few genomic regions showing lower diversity in subcluster B compared with A (in chromosomes 2, 7, 12, and 13). D) Genomewide scan of differentiation between subclusters A and B by sliding window between-population fixation index analysis shows peaks of differentiation corresponding to regions with differences in diversity. Most notable is a large region of chromosome 12 having many windows with between-population fixation index values >0.2 and containing some individual single-nucleotide polymorphisms with fixed differences (Appendix 1 Figure 2, <https://wwwnc.cdc.gov/EID/article/26/8/19-0864-App1.pdf>).



showed differences in levels of diversity are also the most differentiated between the subclusters, most notably the large region of chromosome 12, which has many windows with F_{ST} values exceeding 0.2 (Figure 5, panel D) and contains some individual SNPs with fixed differences (Appendix 1 Figure 4).

Identification of Genomic Loci under Recent Selection in Peninsular Malaysia

To scan for loci that might be under different selection pressures in *P. knowlesi* in Peninsular Malaysia,

we summarized nucleotide site allele frequency spectra by calculating Tajima's D index for all 4,742 genes with ≥ 3 SNPs. Overall, values were negatively skewed (mean -0.86) (Figure 6, panel A); only 215 genes had values >0 , of which only 8 had values >1.0 (Figure 6, panel B). This genomewide pattern is consistent with expectations if long-term population size expansion had occurred. Individual genes with unusually high Tajima's D values (Figure 6, panel B) might be under balancing selection and might be examined separately (Appendix 2 Datasheet 2).

Some genes with high values have orthologs in other malaria parasite species that are likely targets of immunity, including a tryptophan-rich protein (PKNH_1472400, $D = 0.98$), a 6-cysteine protein (PKNH_1254400, $D = 0.61$), an exported protein PHIST (PKNH_0808500, $D = 0.57$), and an MSP7-like protein (PKNH_1265900, $D = 1.15$). However, we found that some other genes with orthologs considered to be targets of immunity in other malaria parasite populations had negative Tajima's D values, including the circumsporozoite protein (*csp*) gene, which had the highest Tajima's D value genome-wide in cluster 1 *P. knowlesi* in Malaysian Borneo (15), as well as the apical membrane antigen 1 gene (*ama1*, $D = -1.35$), the Duffy binding protein α (*DBPA*, $D = -0.89$), and the normocyte binding protein gene (*NBPXa*, $D = -0.42$). These findings indicate that the mode or strength of selection on orthologous targets is not uniform in all malaria parasite populations, including among different *P. knowlesi* subpopulations.

We used the standardized integrated haplotype score $|iHS|$ index as a means of scanning for evidence of genomic regions that are likely to have been affected by recent positive directional selection. Analyzing the full population sample of clinical isolates from Peninsular Malaysia, we observed that 11 SNPs had standardized $|iHS|$ values in the top 0.01%, and examination of the ranges of their extended haplotype homozygosity identified 4 distinct genomic windows of extended haplotypes (Figure 7; Appendix 2 Datasheet 3). Two of these (in chromosomes 1 and 9) spanned across genomic *SICAvar* and *kir* genes that had been masked from SNP calling and analysis. The other 2 windows of extended haplotype homozygosity

did not include *SICAvar* or *kir* genes but covered ≈ 28 kb (11 genes) on chromosome 9 and ≈ 315 kb (81 genes) on chromosome 12. The large region of elevated $|iHS|$ values on chromosome 12 coincides with the region having the highest genomic divergence between cluster 3 population subclusters A and B (Figure 5, panel D), indicating that recent selection on this region has affected part of the *P. knowlesi* population and contributed to the local genetic substructure in Peninsular Malaysia.

Discussion

Genomewide sequence analysis of new clinical isolates has revealed unexpected parasite population structure and evidence of recent selection in *P. knowlesi* in Peninsular Malaysia. On the basis of previous multilocus microsatellite analysis, we expected that genome sequencing of samples from Peninsular Malaysia would reveal a parasite population distinct from those previously described in Malaysian Borneo. This distinction was indeed clearly shown; all samples from Peninsular Malaysia belonged to a genetic population (cluster 3) that is highly divergent genomewide from both of the clusters 1 and 2 in Malaysian Borneo (mean F_{ST} values of 0.32 for cluster 1 and 0.42 for cluster 2). However, the cluster 3 clinical samples from Peninsular Malaysia themselves constituted 3 distinct subpopulations, and the cause of this local population genetic structure needs to be determined. No geographic separation is apparent; each of the three cluster 3 subpopulations was found in overlapping locations, and all were detected from among cases in the hospital that had most samples analyzed. The population structure might reflect >1

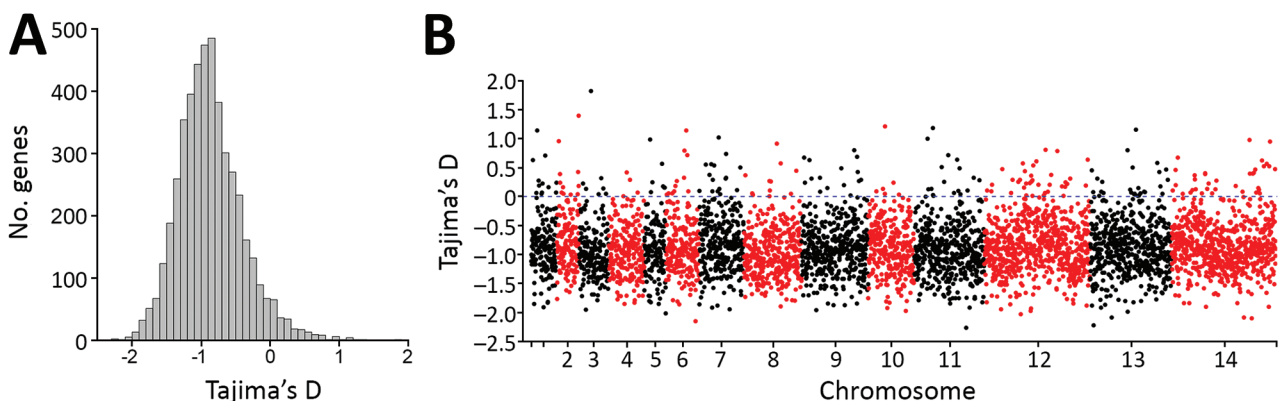
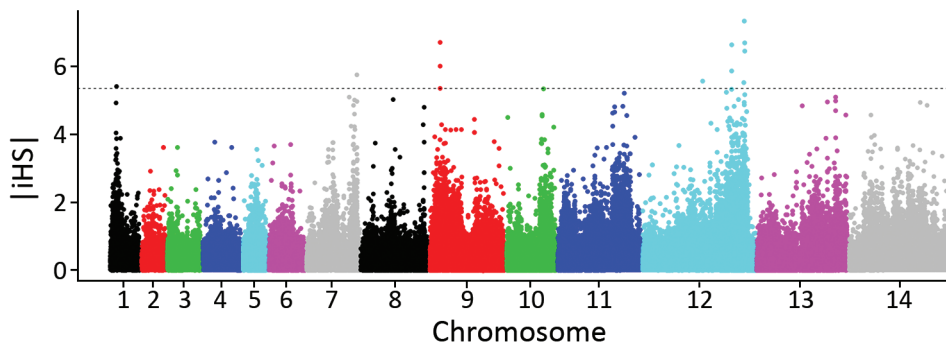


Figure 6. Summary of nucleotide site allele frequency distributions by Tajima's D indices for all 4,742 *Plasmodium knowlesi* genes with ≥ 3 SNPs among the 28 cluster 3 *P. knowlesi* infections in Peninsular Malaysia. A) Overall values were negatively skewed with a mean Tajima's D of -0.86 , consistent with a pattern that would be caused by long-term population size expansion. B) Data for all individual genes show that those with high Tajima's D values are distributed throughout the genome. Some of these genes are likely to be underbalancing selection (individual values for all genes are shown in Appendix 2 Datasheet 2, <https://wwwnc.cdc.gov/EID/article/26/8/19-0864-App2.xlsx>).

Figure 7. Scan for evidence of genomic regions affected by recent positive directional selection in *Plasmodium knowlesi* in Peninsular Malaysia, using the standardized integrated haplotype score |iHS| index. Examination of the ranges of extended haplotype homozygosity for individual single-nucleotide polymorphisms (SNPs) with high |iHS| values identified



4 distinct genomic windows of extended haplotypes (Appendix 2 Datasheet 3, <https://wwwnc.cdc.gov/EID/article/26/8/19-0864-App2.xlsx>). Two of these (in chromosomes 1 and 9) spanned across *SICAvar* and *kir* genes, which were masked from SNP calling, whereas the other 2 did not include *SICAvar* or *kir* genes but covered ≈ 28 kb on chromosome 7 and ≈ 315 kb on chromosome 12. The large region on chromosome 12 is a merged window, consisting of 4 high |iHS| core SNPs with overlapping windows of extended haplotype homozygosity, and coincides with the region of chromosome 12 that has the highest genomic divergence between cluster 3 population subclusters A and B (Figure 5, panel D, <https://wwwnc.cdc.gov/EID/article/26/8/19-0864-F5.htm>).

local zoonotic transmission cycle or could be a sign of recent selection and emergence of a subpopulation of *P. knowlesi* transmitted more effectively between humans.

In Malaysian Borneo, long-tailed macaques are reservoir hosts for the cluster 1 population of *P. knowlesi*, whereas pig-tailed macaques are reservoir hosts for the cluster 2 population (13,14), but whether different reservoir hosts contribute to the parasite population structure we have shown within Peninsular Malaysia is unknown. Microsatellite analysis of *P. knowlesi* in long-tailed macaques from Peninsular Malaysia has indicated that most of them belong to cluster 3, although some samples from long-tailed macaques had indeterminate cluster assignments (13). Our findings underscore the need to sample and genotype parasites from pig-tailed macaques in Peninsular Malaysia, as well as to analyze more samples from long-tailed macaques, to investigate whether the parasite subclusters have different reservoir host species locally.

Genetic subpopulations of *P. knowlesi* in Peninsular Malaysia might also be transmitted by different mosquito species. *P. knowlesi* is transmitted by the *Anopheles* Leucosphyrus group of mosquitoes, which contains a diverse array of species found throughout Southeast Asia (29), including *An. latens*, *An. cracens*, *An. introlatus*, and *An. hackeri*, in which *P. knowlesi* has been detected in Peninsular Malaysia, as well as other species that have been shown to be infected elsewhere (30). *Anopheles* Leucosphyrus group mosquitoes predominantly inhabit forested areas (31,32), so changes to forest areas and ongoing deforestation will affect human exposure. The potential vector species vary in relative abundance among different sampling sites in

Peninsular Malaysia (33–35), but more surveys are required to determine the relative extent to which they transmit *P. knowlesi* and whether they transmit different populations of the parasite (36).

Genomewide scanning revealed discrete regions of divergence between subclusters A and B of *P. knowlesi* cluster 3, in particular a large region on chromosome 12. Interestingly, this region had the strongest evidence of recent directional selection, as indicated by the integrated haplotype score analysis. Moreover, this genomic region did not show evidence of recent selection in Malaysian Borneo (15), so the signature is specific to Peninsular Malaysia and indicates selection to be operating locally.

Even more unexpected is the observation of a separate *P. knowlesi* cluster 3 subpopulation (subcluster C), represented by 3 infections highly related to each other throughout most of the genome. Although less common, clinical cases with this parasite type were identified in different hospitals in 3 different states in Peninsular Malaysia. Population genetic substructure also has been observed in the endemic malaria parasites *P. falciparum* (37) and *P. vivax* (38) in Malaysia, although that observation has been interpreted as indicating fragmented populations that are close to being eliminated. Notable substructure of *P. falciparum* populations also has been observed in Cambodia, probably because of strong selection on locally emerging drug-resistant types in areas where transmission was low (39). Zoonotic *P. knowlesi* populations are probably substructured for other reasons, as previously observed in Malaysian Borneo, where the 2 divergent parasite genetic populations observed in human cases are associated with different reservoir host species (13,14).

Population genomic analysis of *P. knowlesi* so far has mainly focused on parasites from Malaysia, where most reported cases of *P. knowlesi* malaria have been identified. However, cases of *P. knowlesi* malaria in humans have now been reported from all Southeast Asia countries. Whether other local zoonotic subpopulations exist throughout the region or whether all parasites belong to the major genetic populations observed in Malaysia is unknown. Our findings highlight the importance of monitoring population genetic changes in Malaysia and conducting comparable analysis in other areas where *P. knowlesi* has only very recently been realized to occur in humans (40,41).

Acknowledgments

We thank the hospital directors for their cooperation, the medical and nursing staff for obtaining consent and blood samples from malaria patients, and the medical laboratory staff for processing the samples from the Malaysia Ministry of Health hospitals at Kuala Lipis, Gua Musang, Temerloh, Sungai Siput, and Taiping. We thank the Director General of Health in Malaysia for permission to publish this paper. We are grateful to Alfred Amambua-Ngwa for comments on the draft manuscript.

This study was supported by funds from Universiti Malaysia Sarawak (grant no. F05/SpTDG/1447/2016/4), European Research Council (grant no. AdG-2011-294428), and the Biotechnology and Biological Sciences Research Council (London Interdisciplinary Doctoral Training Programme PhD studentship support for S.E.H.).

About the Author

Dr. Hocking completed a PhD in the London Interdisciplinary Doctoral Training Programme (<http://lido-dtp.ac.uk>). Her thesis focuses on sequencing of genomes and transcriptomes to investigate population structure and biology of malaria parasites.

References

- Liu W, Li Y, Learn GH, Rudicell RS, Robertson JD, Keele BF, et al. Origin of the human malaria parasite *Plasmodium falciparum* in gorillas. *Nature*. 2010;467:420–5. <https://doi.org/10.1038/nature09442>
- Loy DE, Plenderleith LJ, Sundararaman SA, Liu W, Gruszczyk J, Chen YJ, et al. Evolutionary history of human *Plasmodium vivax* revealed by genomewide analyses of related ape parasites. *Proc Natl Acad Sci U S A*. 2018;115:E8450–9. <https://doi.org/10.1073/pnas.1810053115>
- Rutledge GG, Böhme U, Sanders M, Reid AJ, Cotton JA, Maiga-Ascofare O, et al. *Plasmodium malariae* and *P. ovale* genomes provide insights into malaria parasite evolution. *Nature*. 2017;542:101–4. <https://doi.org/10.1038/nature21038>
- WHO. World malaria report 2018 [cited 2019 Jun 13]. <https://www.who.int/malaria/publications/world-malaria-report-2018>
- Cox-Singh J, Davis TM, Lee KS, Shamsul SS, Matusop A, Ratnam S, et al. *Plasmodium knowlesi* malaria in humans is widely distributed and potentially life threatening. *Clin Infect Dis*. 2008;46:165–71. <https://doi.org/10.1086/524888>
- Singh B, Kim Sung L, Matusop A, Radhakrishnan A, Shamsul SS, Cox-Singh J, et al. A large focus of naturally acquired *Plasmodium knowlesi* infections in human beings. *Lancet*. 2004;363:1017–24. [https://doi.org/10.1016/S0140-6736\(04\)15836-4](https://doi.org/10.1016/S0140-6736(04)15836-4)
- Shearer FM, Huang Z, Weiss DJ, Wiebe A, Gibson HS, Battle KE, et al. Estimating geographical variation in the risk of zoonotic *Plasmodium knowlesi* infection in countries eliminating malaria. *PLoS Negl Trop Dis*. 2016;10:e0004915. <https://doi.org/10.1371/journal.pntd.0004915>
- Singh B, Daneshvar C. Human infections and detection of *Plasmodium knowlesi*. *Clin Microbiol Rev*. 2013;26:165–84. <https://doi.org/10.1128/CMR.00079-12>
- William T, Jelip J, Menon J, Anderios F, Mohammad R, Awang Mohammad TA, et al. Changing epidemiology of malaria in Sabah, Malaysia: increasing incidence of *Plasmodium knowlesi*. *Malar J*. 2014;13:390. <https://doi.org/10.1186/1475-2875-13-390>
- Cooper DJ, Rajahram GS, William T, Jelip J, Mohammad R, Benedict J, et al. *Plasmodium knowlesi* malaria in Sabah, Malaysia, 2015–2017: ongoing increase in incidence despite near-elimination of the human-only *Plasmodium* species. *Clin Infect Dis*. 2020;70:361–7.
- Lapp SA, Geraldo JA, Chien JT, Ay F, Pakala SB, Batugedara G, et al. MaHPIC consortium. PacBio assembly of a *Plasmodium knowlesi* genome sequence with Hi-C correction and manual annotation of the SICAvax gene family. *Parasitology*. 2018;145:71–84. <https://doi.org/10.1017/S0031182017001329>
- Pain A, Böhme U, Berry AE, Mungall K, Finn RD, Jackson AP, et al. The genome of the simian and human malaria parasite *Plasmodium knowlesi*. *Nature*. 2008;455:799–803. <https://doi.org/10.1038/nature07306>
- Divis PC, Lin LC, Rovie-Ryan JJ, Kadir KA, Anderios F, Hisam S, et al. Three divergent subpopulations of the malaria parasite *Plasmodium knowlesi*. *Emerg Infect Dis*. 2017;23:616–24. <https://doi.org/10.3201/eid2304.161738>
- Divis PC, Singh B, Anderios F, Hisam S, Matusop A, Kocken CH, et al. Admixture in humans of two divergent *Plasmodium knowlesi* populations associated with different macaque host species. *PLoS Pathog*. 2015;11:e1004888. <https://doi.org/10.1371/journal.ppat.1004888>
- Assefa S, Lim C, Preston MD, Duffy CW, Nair MB, Adroub SA, et al. Population genomic structure and adaptation in the zoonotic malaria parasite *Plasmodium knowlesi*. *Proc Natl Acad Sci U S A*. 2015;112:13027–32. <https://doi.org/10.1073/pnas.1509534112>
- Divis PCS, Duffy CW, Kadir KA, Singh B, Conway DJ. Genome-wide mosaicism in divergence between zoonotic malaria parasite subpopulations with separate sympatric transmission cycles. *Mol Ecol*. 2018;27:860–70. <https://doi.org/10.1111/mec.14477>
- Yusof R, Ahmed MA, Jelip J, Ngian HU, Mustakim S, Hussin HM, et al. Phylogeographic evidence for 2 genetically distinct zoonotic *Plasmodium knowlesi* parasites, Malaysia. *Emerg Infect Dis*. 2016;22:1371–80. <https://doi.org/10.3201/eid2208.151885>
- Coatney GR, Collins WE, McWilson W, Contacos PG. The primate malarias. Atlanta: US Department of Health and Human Services; 1971.

19. Moon RW, Hall J, Rangkuti F, Ho YS, Almond N, Mitchell GH, et al. Adaptation of the genetically tractable malaria pathogen *Plasmodium knowlesi* to continuous culture in human erythrocytes. *Proc Natl Acad Sci U S A*. 2013;110:531–6. <https://doi.org/10.1073/pnas.1216457110>
20. Lim C, Hansen E, DeSimone TM, Moreno Y, Junker K, Bei A, et al. Expansion of host cellular niche can drive adaptation of a zoonotic malaria parasite to humans. *Nat Commun*. 2013;4:1638. <https://doi.org/10.1038/ncomms2612>
21. Moon RW, Sharaf H, Hastings CH, Ho YS, Nair MB, Rchiad Z, et al. Normocyte-binding protein required for human erythrocyte invasion by the zoonotic malaria parasite *Plasmodium knowlesi*. *Proc Natl Acad Sci U S A*. 2016;113:7231–6. <https://doi.org/10.1073/pnas.1522469113>
22. Lee KS, Divis PC, Zakaria SK, Matusop A, Julin RA, Conway DJ, et al. *Plasmodium knowlesi*: reservoir hosts and tracking the emergence in humans and macaques. *PLoS Pathog*. 2011;7:e1002015. <https://doi.org/10.1371/journal.ppat.1002015>
23. Pinheiro MM, Ahmed MA, Millar SB, Sanderson T, Otto TD, Lu WC, et al. *Plasmodium knowlesi* genome sequences from clinical isolates reveal extensive genomic dimorphism. *PLoS One*. 2015;10:e0121303. <https://doi.org/10.1371/journal.pone.0121303>
24. Duffy CW, Amambua-Ngwa A, Ahouidi AD, Diakite M, Awandare GA, Ba H, et al. Multi-population genomic analysis of malaria parasites indicates local selection and differentiation at the *gdo1* locus regulating sexual development. *Sci Rep*. 2018;8:15763. <https://doi.org/10.1038/s41598-018-34078-3>
25. Jombart T. adegenet: a R package for the multivariate analysis of genetic markers. *Bioinformatics*. 2008;24:1403–5. <https://doi.org/10.1093/bioinformatics/btn129>
26. Paradis E. pegas: an R package for population genetics with an integrated-modular approach. *Bioinformatics*. 2010;26:419–20. <https://doi.org/10.1093/bioinformatics/btp696>
27. Pfeifer B, Wittelsbürger U, Ramos-Onsins SE, Lercher MJ. PopGenome: an efficient Swiss army knife for population genomic analyses in R. *Mol Biol Evol*. 2014;31:1929–36. <https://doi.org/10.1093/molbev/msu136>
28. Gautier M, Vitalis R. rehh: an R package to detect footprints of selection in genome-wide SNP data from haplotype structure. *Bioinformatics*. 2012;28:1176–7. <https://doi.org/10.1093/bioinformatics/bts115>
29. Sallum MA, Peyton EL, Wilkerson RC. Six new species of the *Anopheles leucosphyrus* group, reinterpretation of *An. elegans* and vector implications. *Med Vet Entomol*. 2005;19:158–99. <https://doi.org/10.1111/j.0269-283X.2005.00551.x>
30. Vythilingam I, Wong ML, Wan-Yusoff WS. Current status of *Plasmodium knowlesi* vectors: a public health concern? *Parasitology*. 2018;145:32–40. <https://doi.org/10.1017/S0031182016000901>
31. Moyes CL, Shearer FM, Huang Z, Wiebe A, Gibson HS, Nijman V, et al. Predicting the geographical distributions of the macaque hosts and mosquito vectors of *Plasmodium knowlesi* malaria in forested and non-forested areas. *Parasit Vectors*. 2016;9:242. <https://doi.org/10.1186/s13071-016-1527-0>
32. Sinka ME, Bangs MJ, Manguin S, Chareonviriyaphap T, Patil AP, Temperley WH, et al. The dominant *Anopheles* vectors of human malaria in the Asia-Pacific region: occurrence data, distribution maps and bionomic précis. *Parasit Vectors*. 2011;4:89. <https://doi.org/10.1186/1756-3305-4-89>
33. Jiram AI, Vythilingam I, NoorAzian YM, Yusof YM, Azahari AH, Fong MY. Entomologic investigation of *Plasmodium knowlesi* vectors in Kuala Lipis, Pahang, Malaysia. *Malar J*. 2012;11:213. <https://doi.org/10.1186/1475-2875-11-213>
34. Vythilingam I, Lim YA, Venugopalan B, Ngui R, Leong CS, Wong ML, et al. *Plasmodium knowlesi* malaria an emerging public health problem in Hulu Selangor, Selangor, Malaysia (2009–2013): epidemiologic and entomologic analysis. *Parasit Vectors*. 2014;7:436. <https://doi.org/10.1186/1756-3305-7-436>
35. Vythilingam I, Noorazian YM, Huat TC, Jiram AI, Yusri YM, Azahari AH, et al. *Plasmodium knowlesi* in humans, macaques and mosquitoes in peninsular Malaysia. *Parasit Vectors*. 2008;1:26. <https://doi.org/10.1186/1756-3305-1-26>
36. Wong ML, Ahmed MA, Sulaiman WYW, Manin BO, Leong CS, Quan FS, et al. Genetic diversity of zoonotic malaria parasites from mosquito vector and vertebrate hosts. *Infect Genet Evol*. 2019;73:26–32. <https://doi.org/10.1016/j.meegid.2019.04.010>
37. Anthony TG, Conway DJ, Cox-Singh J, Matusop A, Ratnam S, Shamsul S, et al. Fragmented population structure of *Plasmodium falciparum* in a region of declining endemicity. *J Infect Dis*. 2005;191:1558–64. <https://doi.org/10.1086/429338>
38. Auburn S, Benavente ED, Miotto O, Pearson RD, Amato R, Grigg MJ, et al. Genomic analysis of a pre-elimination Malaysian *Plasmodium vivax* population reveals selective pressures and changing transmission dynamics. *Nat Commun*. 2018;9:2585. <https://doi.org/10.1038/s41467-018-04965-4>
39. Miotto O, Almagro-Garcia J, Manske M, Macinnis B, Campino S, Rockett KA, et al. Multiple populations of artemisinin-resistant *Plasmodium falciparum* in Cambodia. *Nat Genet*. 2013;45:648–55. <https://doi.org/10.1038/ng.2624>
40. Herdiana H, Irnawati I, Coutrier FN, Munthe A, Mardiaty M, Yuniarti T, et al. Two clusters of *Plasmodium knowlesi* cases in a malaria elimination area, Sabang Municipality, Aceh, Indonesia. *Malar J*. 2018;17:186. <https://doi.org/10.1186/s12936-018-2334-1>
41. Imwong M, Madmanee W, Suwannasin K, Kunasol C, Peto TJ, Tripura R, et al. Asymptomatic natural human infections with the simian malaria parasites *Plasmodium cynomolgi* and *Plasmodium knowlesi*. *J Infect Dis*. 2019;219:695–702. <https://doi.org/10.1093/infdis/jiy519>

Address for correspondence author: David J. Conway, Department of Infection Biology, Faculty of Infectious and Tropical Diseases, London School of Hygiene and Tropical Medicine, Keppel St, London WC1E 7HT, UK; email: david.conway@lshtm.ac.uk

Population Genomic Structure and Recent Evolution of *Plasmodium knowlesi*, Peninsular Malaysia

Appendix 1

Sequencing and SNP Calling Methods

Preparation of libraries for Illumina paired-end short read genome sequencing was performed using 300ng of input DNA from each patient sample with the TruSeq Nano DNA kit (Illumina), with genomic DNA first being sheared into fragments with average size of 550 bp using an M220-Focused Ultrasonicator (Covaris). Library quantification was carried out by quantitative PCR (qPCR) using the KAPA Library Quantification kit for Illumina (KAPA Biosystems) and library quality was assessed with the Agilent High Sensitivity DNA kit on the Agilent Bioanalyser (Agilent). Any samples showing significant primer dimer content or containing less than 4nM of DNA by qPCR were not processed for sequencing. Samples passing quality criteria were normalized to 4nM and pooled equimolar in batches of no more than eight. Library pools were denatured and diluted to a final concentration of 15pM and spiked with 1% PhiX.

Paired-end sequencing was performed on an Illumina MiSeq using 600-cycle v3 MiSeq reagents with a read length of 300 bp, and raw data were generated in FASTQ format, with FastQC (<http://www.bioinformatics.babraham.ac.uk/projects/fastqc/>) used to assess quality of the short reads and inform the trimming to remove low quality base calls. Numbers of short reads per sample ranged from 3.2 million to 9.8 million, and the GC content of each sample was checked, so that any straying from the expected 38% GC content of the *Plasmodium knowlesi* genome was inspected in case of potential contamination.

Short reads were first trimmed with Trimmomatic v0.3.2 using default parameters (1), and then aligned to the *P. knowlesi* PKNH version 2.0 reference genome with BWA-MEM (2). Mapped reads were converted to bam format, sorted, and indexed using samtools version 1.3.1

(3). Reads originating from PCR duplicates were removed using Picard (<https://broadinstitute.github.io/picard>). Average read depth was calculated using SAMtools and samples with an average coverage of less than 20x were excluded from further analysis.

The first round of SNP calling was performed on each sample independently. SNPs were initially marked using samtools mpileup run with the following flags: `-B -I -Q 23 -d 2000 -C 50`, and marked SNPs were then called using `bcftools call -m -v` and filtered using `vcftutils.pl varFilter -d 10 -D 2000`. The resulting per-sample SNP lists were then filtered, and positions with a read depth of less than 30x were discarded. The SNPs for each sample were then compiled into a single file, resulting in a ‘unique SNP list’ representing the *P. knowlesi* population, containing SNP positions and alternate bases. Any SNPs falling within subtelomeric regions or *kir* and *SICAvar* gene regions as noted above were filtered out of the unique SNP lists using bedtools intersect v2.27.0 (4). A second round of SNP calling and filtering was then implemented using custom made Perl scripts (5) to make the major genotype call at each SNP position for each sample. SNP positions that had 50:50 split in mixed base calls for a particular sample were uncalled and scored as ‘N’. Positions that had data missing in more than 10% of the infection samples were not analyzed.

Parts of the genome are difficult to uniquely map short reads to, and were therefore masked from analysis, including the subtelomeres and the multi-copy *kir* and *SICAvar* gene families and low complexity intergenic regions between these. Boundaries of subtelomeric regions were defined as in previous analysis (6), while *kir* and *SICAvar* genes were identified using the gene search function of PlasmoDB (www.plasmodb.org) and verified by inspecting the *P. knowlesi* annotation Embl files in Artemis (7). In genomic regions where several polymorphic genes belonging to *kir* and *SICAvar* families occurred sequentially, the masked region was extended to include all genes and intergenic sequence, and extended on each side until the first SNP called after the final masked gene in that region.

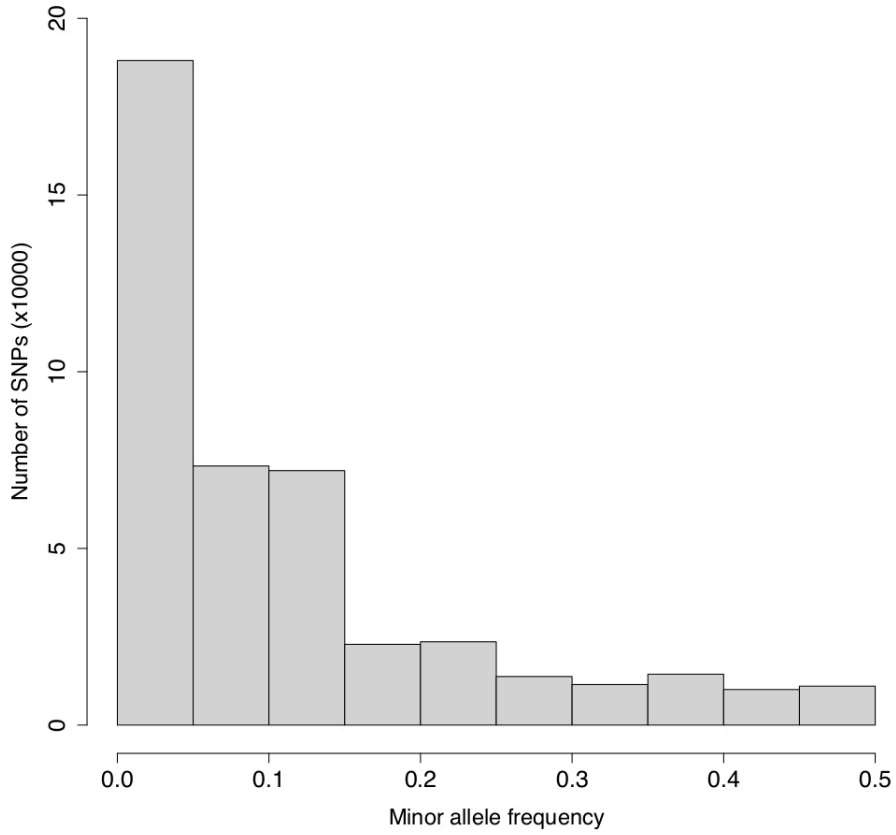
References

1. Bolger AM, Lohse M, Usadel B. Trimmomatic: a flexible trimmer for Illumina sequence data. *Bioinformatics*. 2014;30:2114–20. [PubMed https://doi.org/10.1093/bioinformatics/btu170](https://doi.org/10.1093/bioinformatics/btu170)
2. Li H, Durbin R. Fast and accurate short read alignment with Burrows-Wheeler transform. *Bioinformatics*. 2009;25:1754–60. [PubMed https://doi.org/10.1093/bioinformatics/btp324](https://doi.org/10.1093/bioinformatics/btp324)

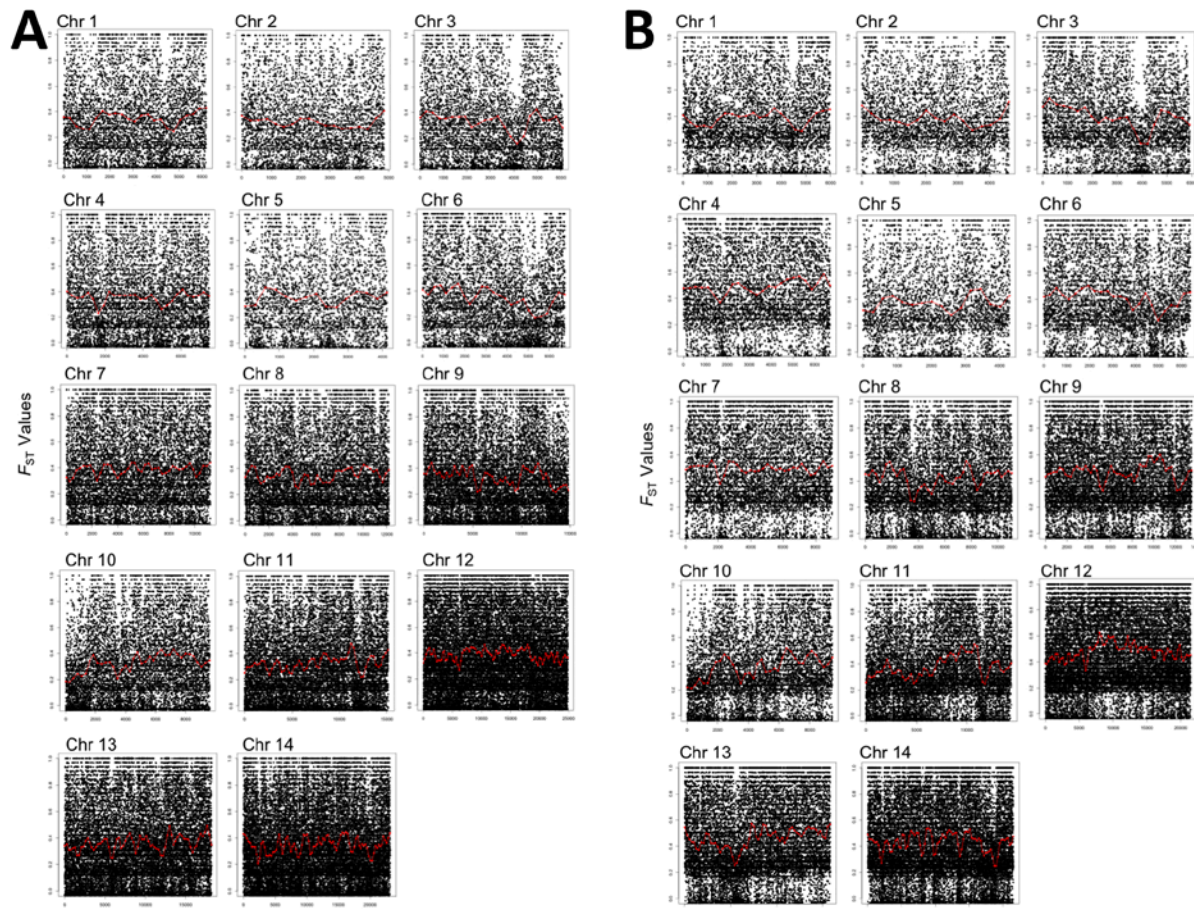
3. Li H, Handsaker B, Wysoker A, Fennell T, Ruan J, Homer N, et al.; 1000 Genome Project Data Processing Subgroup. The Sequence Alignment/Map format and SAMtools. *Bioinformatics*. 2009;25:2078–9. [PubMed https://doi.org/10.1093/bioinformatics/btp352](https://doi.org/10.1093/bioinformatics/btp352)
4. Quinlan AR, Hall IM. BEDTools: a flexible suite of utilities for comparing genomic features. *Bioinformatics*. 2010;26:841–2. [PubMed https://doi.org/10.1093/bioinformatics/btq033](https://doi.org/10.1093/bioinformatics/btq033)
5. Assefa S, Lim C, Preston MD, Duffy CW, Nair MB, Adroub SA, et al. Population genomic structure and adaptation in the zoonotic malaria parasite *Plasmodium knowlesi*. *Proc Natl Acad Sci U S A*. 2015;112:13027–32. [PubMed https://doi.org/10.1073/pnas.1509534112](https://doi.org/10.1073/pnas.1509534112)
6. Divis PCS, Duffy CW, Kadir KA, Singh B, Conway DJ. Genome-wide mosaicism in divergence between zoonotic malaria parasite subpopulations with separate sympatric transmission cycles. *Mol Ecol*. 2018;27:860–70. [PubMed https://doi.org/10.1111/mec.14477](https://doi.org/10.1111/mec.14477)
7. Rutherford K, Parkhill J, Crook J, Horsnell T, Rice P, Rajandream MA, et al. Artemis: sequence visualization and annotation. *Bioinformatics*. 2000;16:944–5. [PubMed https://doi.org/10.1093/bioinformatics/16.10.944](https://doi.org/10.1093/bioinformatics/16.10.944)

Appendix 1 Table. Origins and primary data on the 28 *Plasmodium knowlesi* clinical infection samples from Peninsular Malaysia with genomewide sequences obtained in this study

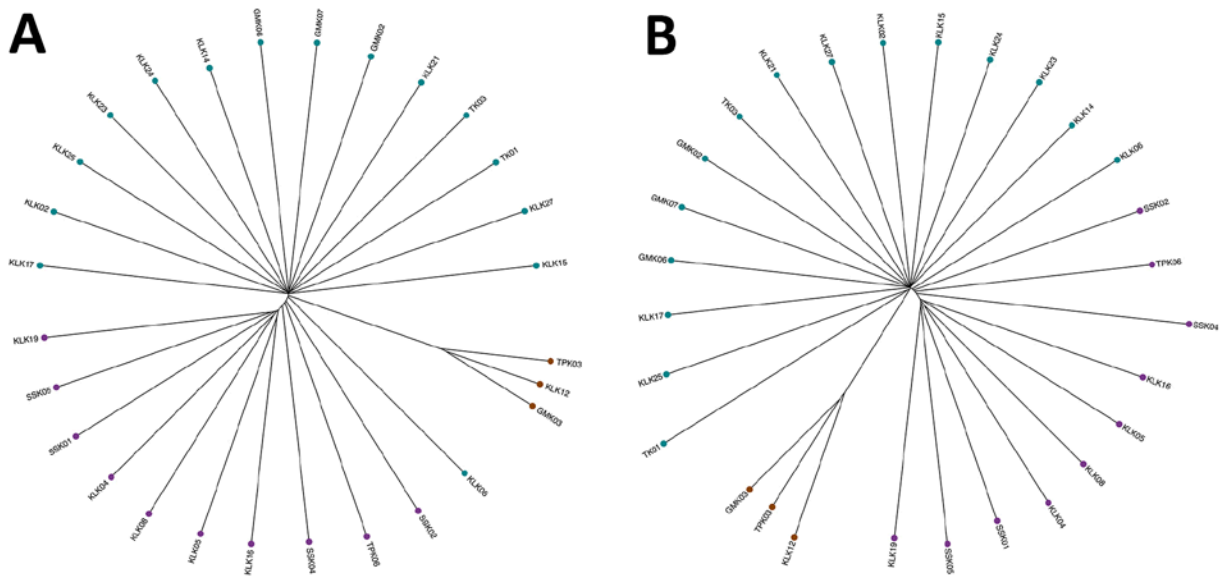
Infection sample	Location	Date collected	Parasitemia μl^{-1} blood	Total reads ($\times 10^6$)	Genomewide mean read depth coverage	ENA accession no.
GMK02	Gua Musang	2016 Nov 5	88,164	5.8	47x	ERS3517629
GMK03	Gua Musang	2017 Feb 19	16,480	5.6	40x	ERS3517630
GMK06	Gua Musang	2018 Jan 15	98,800	8.7	74x	ERS3517631
GMK07	Gua Musang	2018 Jan 21	12,900	7.9	66x	ERS3517632
KLK02	Kuala Lipis	2016 Jul 29	1,932	3.2	40x	ERS3517633
KLK04	Kuala Lipis	2016 Aug 9	50,938	4.0	32x	ERS3517634
KLK05	Kuala Lipis	2016 Sep 18	27,251	5.0	36x	ERS3517635
KLK06	Kuala Lipis	2016 Oct 23	661,875	5.8	43x	ERS3517636
KLK08	Kuala Lipis	2017 Jan 30	84,400	3.6	91x	ERS3517637
KLK12	Kuala Lipis	2017 Mar 2	7,236	3.6	27x	ERS3517638
KLK14	Kuala Lipis	2017 Apr 9	33,060	5.8	46x	ERS3517639
KLK15	Kuala Lipis	2017 Apr 12	136,408	5.4	37x	ERS3517640
KLK16	Kuala Lipis	2017 May 17	13,756	5.4	37x	ERS3517641
KLK17	Kuala Lipis	2017 May 19	22,554	5.8	44x	ERS3517642
KLK19	Kuala Lipis	2017 Jul 11	46,035	4.4	37x	ERS3517643
KLK21	Kuala Lipis	2017 Aug 28	60,950	4.5	39x	ERS3517644
KLK23	Kuala Lipis	2017 Feb 25	23,288	8.3	71x	ERS3517645
KLK24	Kuala Lipis	2017 Dec 7	141,069	5.7	47x	ERS3517646
KLK25	Kuala Lipis	2018 Jan 16	54,352	3.7	32x	ERS3517647
KLK27	Kuala Lipis	2018 Jan 19	69,160	7.8	64x	ERS3517648
SSK01	Sungai Siput	2016 Sep 30	6,027	8.8	40x	ERS3517649
SSK02	Sungai Siput	2016 Dec 2	2,763	7.6	62x	ERS3517650
SSK04	Sungai Siuit	2017 Jan 25	6,750	3.6	22x	ERS3517651
SSK05	Sungai Siput	2017 Mar 7	6,750	3.8	30x	ERS3517652
TK01	Temerloh	2016 Aug 2	3,806	4.4	21x	ERS3517653
TK03	Temerloh	2017 Feb 21	10,323	6.0	49x	ERS3517654
TPK03	Taiping	2017 Aug 30	4,000	9.8	55x	ERS3517655
TPK06	Taiping	2017 Nov 15	12,494	8.8	74x	ERS3517656



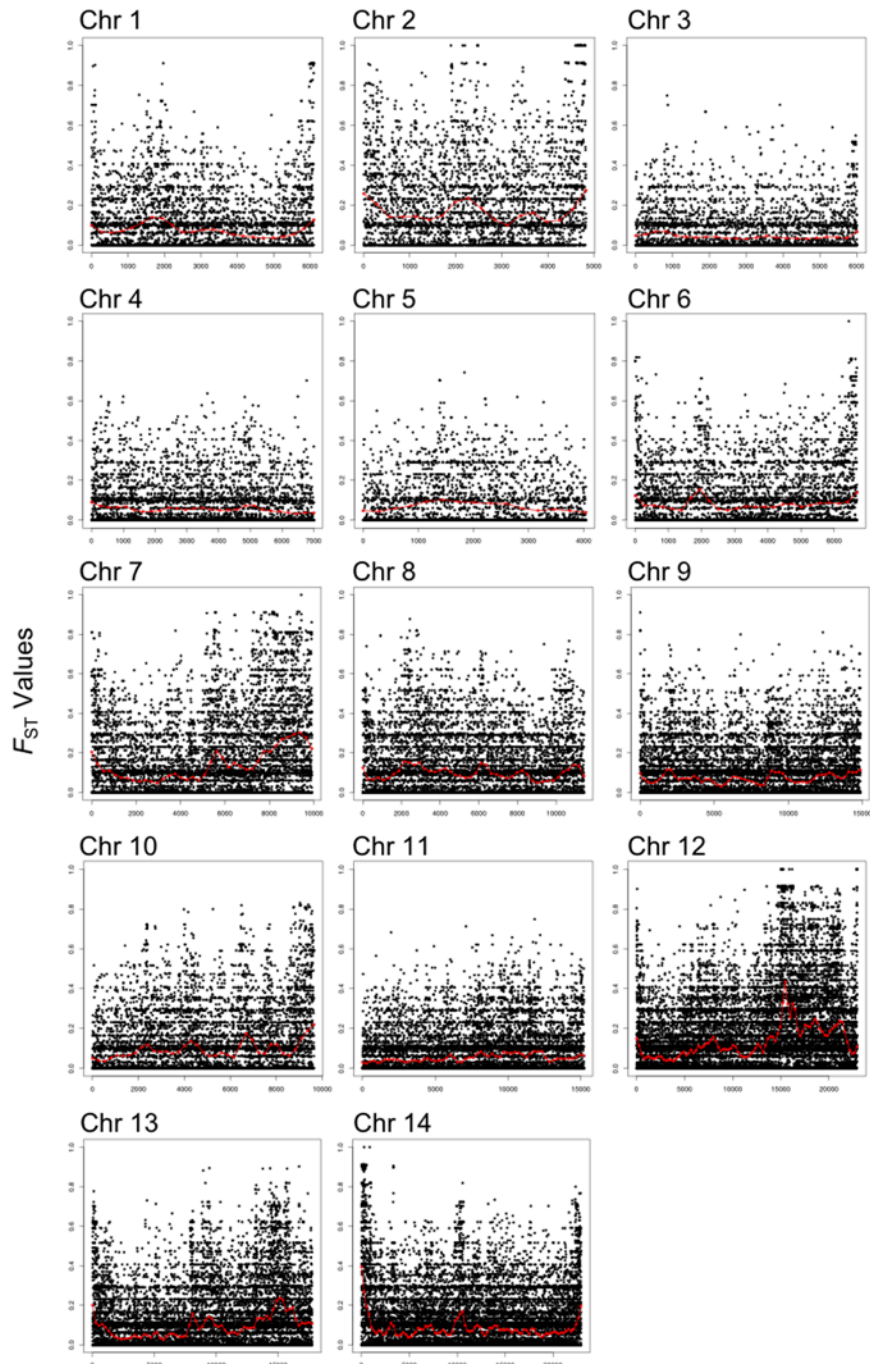
Appendix 1 Figure 1. Minor allele frequency distribution of all SNPs analyzed in *Plasmodium knowlesi* cluster 3 (sample of 28 clinical isolates from Peninsular Malaysia).



Appendix 1 Figure 2. Genomewide plots of F_{ST} values of allele frequency divergence for all individual SNPs, for comparisons between the *Plasmodium knowlesi* population in Peninsular Malaysia (cluster 3) and each of the two genetic populations in Malaysian Borneo (clusters 1 and 2). A. cluster 3 versus cluster 1. B. Cluster 3 versus cluster 2. Comparison between *P. knowlesi* cluster 1 and 2 is not shown as this was published previously (Divis PCS, Duffy CW, Kadir KA, Singh B, Conway DJ. Genomewide mosaicism in divergence between zoonotic malaria parasite subpopulations with separate sympatric transmission cycles. *Mol Ecol.* 2018;2:860–70). F_{ST} values shown for all individual SNPs with MAF >10%, comparing between *P. knowlesi* cluster 3 in Peninsular Malaysia and cluster 2 in Malaysian Borneo. In red are shown the means for overlapping windows of 500 SNPs (step size of 250 SNPs along chromosomes).



Appendix 1 Figure 3. Neighbor-Joining trees (NJ) indicating clustered relatedness among 28 new clinical isolates within *Plasmodium knowlesi* cluster 3. A. Distance matrix based on all SNPs genome-wide. B. Distance matrix based on SNPs genome-wide excluding those on chromosome 12.



Individual SNPs and midpoints of sliding windows along each chromosome

Appendix 1 Figure 4. Genomewide plots of F_{ST} values of allele frequency divergence for all individual SNPs, for comparisons between the two largest subpopulations of *Plasmodium knowlesi* cluster 3 (subclusters A and B) within the population in Peninsular Malaysia. F_{ST} values shown for all individual SNPs with MAF >10%, comparing between subclusters A and B of *P. knowlesi* cluster 3 within Peninsular Malaysia. In red are shown the means for overlapping windows of 500 SNPs (step size of 250 SNPs along chromosomes).